QUANTITATIVE RISK ASSESSMENT FOR HYDROGEN SYSTEMS: MODEL DEVELOPMENT AND VALIDATION

Dutta, Kanchan, David, Robert, Liang, Zhe
Hydrogen Technologies, Canadian Nuclear Laboratories, 286 Plant Rd, Chalk River, Ontario, K0J 1J0, Canada, kanchan.dutta@cnl.ca, robert.david@cnl.ca, zhe.liang@cnl.ca

ABSTRACT

Quantitative Risk Assessment (QRA) is a risk-informed approach that considers past performances and the likelihood of events and distinguishes must-haves from nice-to-haves. Following the approach applied for the HyRAM code, developed by the Sandia National Laboratories, a QRA toolkit for hydrogen systems was developed using MATLAB by Canadian Nuclear Laboratories (CNL). Based on user inputs for system components and their operating parameters, the toolkit calculates the consequence of a hydrogen leak from the system. The fatality likelihood can be estimated from the severity of a person's exposure to radiant heat flux (from a jet fire) and overpressure (from an explosion). This paper presents a verification and validation exercise by comparing the CNL model predictions with the HyRAM code and available experimental data, including a QRA case study for a locomotive. The analysis produces risk contours recommending personnel (employees/public) numbers, time spent, and safe separation distances near the incident (during maintenance or an accident). The case study demonstrated the importance of hydrogen leak sensors' reliability for leak detection and isolation. The QRA toolkit calculates a more practical value of the safe separation distance for hydrogen installations and provides evidence to support communication with authorities and other stakeholders for decision-making.

1. INTRODUCTION

Hydrogen is well known as a flammable and explosive gas. Therefore, an accident resulting from a hydrogen leak-related incident can have a significant safety and economic consequences. Raising awareness about hydrogen safety among people, communities, and organizations while developing and using new hydrogen-related technologies is one of the recommendations of Natural Resources Canada's Hydrogen Strategy for Canada [1]. The Canadian Hydrogen Installation Code (CHIC) [2], approved by the Interprovincial Gas Advisory Council and adopted by some Canadian provinces, mandates installation requirements for hydrogen systems. The Code states, "A risk assessment shall be completed" that identifies and evaluates risks to develop a mitigation plan.

A risk assessment process systematically analyzes the hydrogen system and brainstorms what could go wrong. The assessment then evaluates current controls and mitigation measures to foresee if they can prevent the incident from turning into an accident with damaging consequences due to thermal and pressure impacts. The assessment could be qualitative, semi-quantitative or quantitative. A team of subject matter experts typically carries out qualitative or semi-quantitative assessments. QRA is a risk-informed approach that considers past performances, probabilities of events leading to potential accidents, and risk reduction from mitigation measures. QRA considers multiple hazard scenarios in the evaluation, not just the worst-case scenario. Contrarily, a risk-based approach considers the harm caused by the worst possible outcome of an incident/accident to determine hazard distances.

In 2015, Sandia National Laboratories released its first version of the Hydrogen Risk Assessment Model (HyRAM) software. HyRAM integrates deterministic and probabilistic models to ascertain the likelihood and frequency of an event (e.g., jet fire or explosion) following a hydrogen leak [3]. The event's consequence is quantified using validated models to calculate the physical outcomes (e.g., radiative heat flux or overpressure) of an incident/accident and using probit equations to characterize the impacts on the people in the vicinity of the incident. HyRAM uses generic probabilities for equipment failures for different system components and ignition [4]. These probabilities determine the annual frequencies of ignition events in a hydrogen system. Low event frequencies and mitigation measures can potentially reduce the risk and the safe separation distance.

Skjold et al. [5] combined consequence assessments from Gexcon's FLACS-Hydrogen and HyRAM event frequencies to generate 3D risk contours for explosion pressure and radiation loads for a hypothetical hydrogen filling station. Gye et al. [6] conducted a quantitative risk assessment of an urban hydrogen refuelling station using multiple scenarios. The assessment gave unacceptable risks from low frequency significantly damaging incidents. The authors concluded that applying immediate detection and isolation sensors could decrease the frequency and amount of leakage from the hydrogen equipment. Ehrhart et al. [7] conducted a risk assessment and ventilation modelling for hydrogen vehicle repair garages, where HyRAM was used for components failure frequencies and ignition probabilities. Hirayama et al. [8] used HyRAM to evaluate safety distances for hydrogen vehicle fuel dispensers. The authors obtained different safety distances for jet fires, explosions, and flash fires that would contribute to the decision-making process used to determine proper safety distances for hydrogen dispensers.

At Canadian Nuclear Laboratories (CNL), a QRA toolkit is being developed using MATLAB, adopting the same risk assessment approach implemented in HyRAM. The primary motivation for this toolkit was to utilize the results of Computational Fluid Dynamics modeling and experiments developed at CNL for risk quantification. The toolkit also facilitates modeling systems containing other gas blends (hydrogen and methane). This paper presents the QRA results using the toolkit for a hydrogen fuel cell locomotive operated in Canada. The toolkit outputs were validated with HyRAM results and literature data. The analysis used representative piping and instrumentation diagrams to define the hydrogen system for the locomotive. Multiple leak sizes similar to those in HyRAM were considered to determine the risk to the locomotive occupants and the safe separation distance. Sensitivity analyses were conducted to demonstrate the importance of mitigation measures (that is, leak detection and isolation) and routine scheduled preventive maintenance of the system.

2. QRA METHODOLOGY

2.1 Events of Hydrogen Leaks

Compressed gaseous hydrogen is commonly stored in tanks. Most failures lead to hydrogen leaks from these tanks or attached components (e.g., pipes, fittings, pressure relief devices, filters, flanges, or valves). The leak can result in the formation of combustible hydrogen-air mixtures. A hydrogen release in confined or semi-confined geometries is a significant safety issue due to the potential accumulation and explosion. An unconfined release can also become a safety concern when hydrogen burns at the leak, forming a jet fire, or the leak occurs within an obstructed area, causing an explosion. The following event sequence diagram (Figure 1) could be used for any leak incident [3]. Four possible aftermaths (hereafter referred to as "events") from the leak are shown in Figure 1.
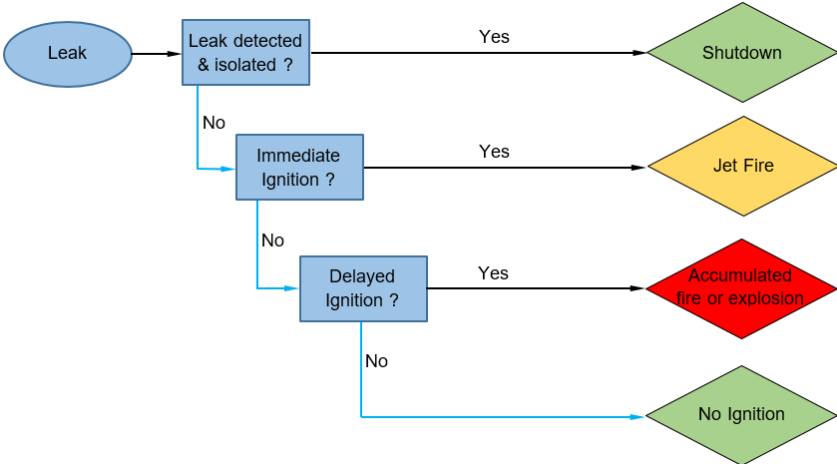

Figure 1: Event sequence diagram following a hydrogen leak.

2.2 Physics Models: Event Outcomes Quantification

Several physics models and correlations could be used for calculating the jet plume dimension (length, diameter, and trajectory), radiant heat flux from the flame, and overpressure-impulse effects. Discrete levels of event outcomes (heat flux, overpressure) are used to determine whether they are benign or have damaging impacts on people and infrastructures. This deterministic approach [9] calculates the radius of influence (hazard distance) up to where the heat flux and overpressure effects cause damage to people and structures.

Notional nozzles are used to calculate the effective diameter, velocity, and thermodynamic state of the under-expanded jet [10]. At the onset of a leak from a pressurized tank, the flow is choked at the jet exit with the exit pressure considerably greater than atmospheric pressure, producing an under-expanded jet. The mass is conserved between the flow through the leak orifice and the flow through the notional nozzle. The mass flow rate, an outcome of the mass conservation at the orifice and the nozzle, determines ignition event probabilities (Section 3.1.2) and the radiative heat flux (discussed below).

In the flame radiation heat flux model [11], the flame properties of importance are the visible flame length, total radiative power emitted from the flame, and total heat released due to chemical reaction. Only a fraction of the total heat released by the chemical reaction is radiated to the surroundings, known as the radiant fraction. The product of this fraction and the total heat released by the chemical reaction is the total radiative power emitted from the flame. The total heat released by the chemical reaction is a product of the mass flow rate and the heat of combustion. The heat flux is calculated at a given location using a weighted multi-point source method [12], applied to a jet flame with buoyancy correction.

The QRA case study in Section 3 assumes a leak occurs in an open space. If the leak size is large and a jet fire is not initiated immediately, a significant amount of explosive mass can be formed in the vicinity of the leak [3]. Delayed ignition of this mass can cause damage to humans and structures. A conservative approach is used to estimate the overpressure and impulse of the explosion in this case of delayed ignition of jet releases. The overpressure and impulse are a function of the position of the occupant and explosive energy, which depends on the total explosive mass of hydrogen, the heat of combustion, and the ground reflection factor (assumed to be 2). This explosive energy is used to scale the distance from the origin into a dimensionless distance and calculate the scaled overpressure and impulse from the Baker-Strehlow-Tang (BST) blast curves [13]. The location where the hydrogen concentration is halfway between the lower and the upper flammability limits along the jet plume axis is assumed to be the origin of the explosion.

2.3 Frequencies

2.3.1 Random Component Leak and Incident/Accident Frequencies

Ehrhart et al. [3] estimated the annual frequency of a leak for five leak sizes of 0.01%, 0.1%, 1%, 10%, or 100% of the pipe flow area (based on inner pipe diameter). For all leak sizes, the contribution to the leak frequency is made by random component leaks (e.g., random leaks in pipes, vessels, compressors). The annual frequency of random leaks for each leak size (k) is the product of the total number of ith component ($\sum N_i$) in the system and the leak frequency of the ith component. The annual random leak frequencies of various leak sizes for different components were assembled from generic data from offshore oil, process chemical, and nuclear power industries [3]. For example, for vessels, the annual leak frequencies for leak sizes of 0.01%, 0.1%, 1%, 10%, or 100% of pipe flow area are 1.4×10^{-6}, 1.2×10^{-6}, 7.9×10^{-7}, 4.5×10^{-7}, and 2.3×10^{-7}, respectively [3]. The value for each leak size is the median for the lognormal distribution for that leak size (k) in the component (i). The total random frequency for a leak size k for all components N_i is given by:

$$f_{random,k} = \sum_i (N_i \times f_{random,i,k}) \tag{1}$$

In addition to the random components leak frequencies, during refueling, the 100% leak size includes drive-off incidents, tank overpressure during refueling, and shutdown failures [3]. The frequency of

accidents imparting impact damages to the components (e.g., during head-on vehicle collisions, rail vehicle derailments, vehicle toppling over) will also contribute to the frequency of 100% leak size.

2.3.2 Event Frequencies

Each leak size defined in Section 2.3.1 can result in one of the four events depicted in Figure 1. Each leak size is associated with an initial mass flow rate at the inception of the leak. If not isolated, the probability of immediate and delayed ignition depends on the hydrogen leak rates. The probabilities for immediate and delayed ignitions are listed in Table 1. They are defined according to the hydrogen leak rates provided in Reference [4].

The total random component leak frequency (for all components) at each leak size could be calculated using equation (1). The frequencies of the events (Figure 1) at each leak size are the product of this total leak frequency and the probability of each event determined as follows:

- Shutdown: A leak, if detected and isolated, will cause no harm. This shutdown event depends on the probability of detecting and isolating a leak ($P_{detec} = 0.9$ was used in this case study). The probability of no shutdown, $P_{no\ detec} = (1 - P_{detec})$, determines the frequency of other events if a leak is not isolated.
- Jet fire: The probably for jet fire at each leak size is a product of immediate ignition probability ($P_{immediate}$, Table 1) and $P_{no\ detec}$.
- Explosion: A delayed ignition may occur when immediate ignition does not take place. The probability of no immediate ignition is $P_{no\ immediate} = 1 - P_{immediate}$. The probability of the delayed ignition at a leak size is the product of delayed ignition probability ($P_{delayed}$, Table 1), $P_{no\ immediate}$ and $P_{no\ detec}$.
- No ignition: When a leak is not isolated, and the leak does not ignite, hydrogen disperses away. The probability of no ignition is one minus the sum of all other event probabilities.

Table 1. Ignition probabilities for hydrogen at different mass flow rates [4].

H_2 release rate (kg s^{-1})	Ignition probability	
	$P_{immediate}$	$P_{delayed}$
<0.125	0.008	0.004
0.125–6.25	0.053	0.027
>6.25	0.230	0.120

2.4 Consequences of Event Outcomes

The consequences (c_i) of an accident could be expressed as the number of fatalities or repair costs in a specific period. The probability of fatality of a person depends on the location of the person (distance from the leak and epicentre of an event outcome, such as overpressure). The severity of the consequence depends on the radiant heat flux intensity (causing burn damage) and overpressure (causing damage by the impact of flying objects/debris or organ damage) received at a given location. The damage caused by heat flux and overpressure effects is calculated using the probit models [14]. The use of probit models is the probabilistic approach [9] to determine the probability of fatality of an occupant exposed to heat flux and overpressure impulse. The fatality probability is used to calculate the risk metrics and then compared with their maximum tolerable values for acceptance.

The probability of a fatality ($P_{fatality}$) is given by Equation (2), which evaluates the standard normal cumulative distribution function at the value (Y), with a mean value, $\mu = 5$, and standard deviation, $\sigma = 1$, established by the appropriate probit model.

$$P_{fatality} = F(Y | \mu = 5, \sigma = 1) \qquad (2)$$

The parameter Y in Equation (2) depends on the heat flux intensity (I in W·m^{-2}) and exposure time (t in s) for damage by jet fire, or peak overpressure (P_s in Pa) and impulse (i in Pa·s) for damage by explosion. There are multiple probit models for each damaging scenario. The mean and standard deviation values are based on how the probit equation was originally developed.

For damage by a hydrogen jet fire, LaChance et al. [15] recommended using the Eisenberg model, Equation (3).

$$\text{Eisenberg, } Y = -38.48 + 2.56 \ln\left(I^{4/3}t\right) \qquad (3)$$

For damage by an explosion, the TNO probit model, Equation (4), is recommended [15].

$$\text{TNO Head Impact, } Y = 5 - 8.49 \ln\left(\frac{2430}{P_s}\right) + \frac{4}{(P_s\,i)} \qquad (4)$$

In addition to internal organ (e.g., lungs, eardrum) damage, overpressure can also cause indirect damage by head impact by flying debris during the collapse of structures. These indirect effects from overpressure represent the most critical concern for people [15]. Table 2 lists some threshold values for the heat flux and overpressure that can cause damage [15].

It should be noted that even if the outcome of a leak may lead to a damaging heat flux or overpressure, the ultimate fatality rate depends on the probability of that outcome of an event (immediate, delayed, or no ignition, Figure 1), along with system parameters and peoples' locations.

Table 2 Damage to humans from radiative heat flux and overpressure

Heat flux ($kW \cdot m^{-2}$)	Consequences	Overpressure (kPa)	Consequences
< 1.6	No harm for long exposures	13.8	Eardrum rupture threshold
4–5	First degree burn (in 20 s)	48.3	Internal injuries threshold
9.5	Second-degree burn	82.7–103.4	Lung haemorrhage threshold

2.5 Risk Metrics

A risk is a possibility of a hazard turning into injury or loss. It is a combination of the severity of the consequence (c_i) of an accident scenario and the probability (p_i) of the scenario [3]:

$$\text{Risk} = \sum_i c_i \times p_i \qquad (5)$$

Risk can also be expressed as the product of frequencies (f_i) and consequences across all scenarios. The frequency (f_i) is analogous to the probability (p_i). The product of the frequency of an event (Figure 1) at a leak size (for all components) and the associated fatality/damage (for all occupants) is the fatalities per leak size per year. The sum of these fatalities for all leak sizes gives the total loss of life in the defined population per year. The common risk-related metrics could be calculated based on Potential Loss of Life (PLL) and Average Individual Risk (AIR) [3]. PLL is the expected number of fatalities per system per year. It is the total number of fatalities in a hydrogen system in a given period from a population in the vicinity of the system. It is calculated as the sum of the products of the number of fatalities at each leak size and the annual frequency of the event (causing these fatalities, e.g., jet fire, explosion, etc.) at that leak size. For example, there will be one PLL value for the immediate ignition and one for the delayed. The sum of these two PLL values will be the total PLL.

AIR is the expected number of fatalities per exposed individual. It considers the average number of hours ($N_{h/person}$) that an occupant spends on-site:

$$\text{AIR} = \frac{\text{PLL} \times N_{h/person}}{N_{persons} \times 365 \text{ days} \times 24 \text{ h}} \qquad (6)$$

The risk metric calculated using Equation (6) is compared to pre-defined risk criteria by the International Energy Agency, AIR $\leq 1 \times 10^{-4}$ yr^{-1} for a worker or $\leq 1 \times 10^{-5}$ yr^{-1} for a member of the public [14].

3. QRA CASE STUDY: HYDROGEN LOCOMOTIVE

A case study was carried out for a locomotive housing the hydrogen system (i.e., storage tanks, piping, instruments, cooling system, and refueling system). Table 3 summarizes the input parameters for the case study; an industry partner provided the data. A leak can happen during refuelling with at least one

person nearby (in the vicinity of the leak). As an outcome of a leak, the jet flame could be horizontal or vertical (or at any angle in between). Only horizontal flame has been considered for calculating risks and the safe separation distance. But the separation distance is represented by a radius around the leak that accounts for all possible flame orientations relative to the horizontal axis.

Table 3 Parameters used for the case study, data provided by an industry partner

Components	Values	Gas storage and ambient conditions	Values
Pipe straight equivalent length (m)	30.5	Gas pressure (bar)	350
Pipe outer diameter (OD, inch)	0.75	Gas temperature (°C)	15
Pipe wall thickness (inch)	0.109	Ambient temperature (°C)	25
Cylinders (#)	10	Humidity (%)	75
Filters (#)	8	CO_2 conc. in air (ppm)	400
Flanges (#)	1	Atmospheric pressure (bar)	1.013
Hoses (#)	2	Planck-mean absorption coefficient for an optically thin flame	0.23
Joints (#)	142	**Vehicle details and usage**	**Values**
Valves (#)	47	Locomotive length (m)	6.3
Instruments (#)	27	Locomotive width (m)	1.6
Probability of detecting and isolating leak	0.9	No. of H_2 locomotive vehicle (#)	1
Exposure time to radiant heat flux (s)	60	No. of times the FCV is fuelled (# / day)	1
No. of leak sizes (#)	5	No. of operating days (#)	365
Leak sizes (% of flow area)	0.01, 0.1, 1, 10, and 100	**Occupant**	**Values**
		No. of occupants (#)	1
		No. of working h / week	35
		No. of working weeks / year	52

3.1 QRA Results

3.1.1 Physics Model

Figure 2 shows the contour plots of heat flux, overpressure, and impulse generated from jet fire or explosion events for leak sizes of 1%, 10%, and 100% from a ¾″ OD line containing H_2 at 350 bar. The threshold used for heat flux is that no injury is caused for prolonged exposure (≤ 2 kW·m^{-2}). The overpressure threshold is 10 kPa, which is required to knock down a person. Both overpressure and impulse effects spread spherically from their origin (Section 2.2). The impulse effects are found to be negligible below 1% leak size. Table 4 summarizes the hazard distances based on heat flux and overpressures. These hazard distances do not consider the likelihood of an event following a leak. These hazard distances have been validated with HyRAM physics models.

Table 4 Hazard distances based on heat flux and overpressures

Leak size [% of flow area]	Heat Flux effects		Overpressure effects	
	Threshold [kW·m^{-2}]	Hazard distance [m]	Threshold [kPa]	Hazard distance [m]
0.01		0.3		0.5
0.1		1		1.6
1	2	3.5	10	5.3
10		12		16.6
100		43		52.6

In a risk-based approach to risk assessment, these hazard distances extending several times the maximum locomotive dimension (1.6 m × 6.3 m) are used as prescriptive separation distances. However, a risk-informed approach in QRA also considers the probability of events. While these events could be damaging, the fatality risk remains low due to the low occurrence probability of these events. Subsequent sections elaborate the consideration of probabilities and resulting event frequencies on fatalities and risks and the sensitivity of these parameters on separation distance.
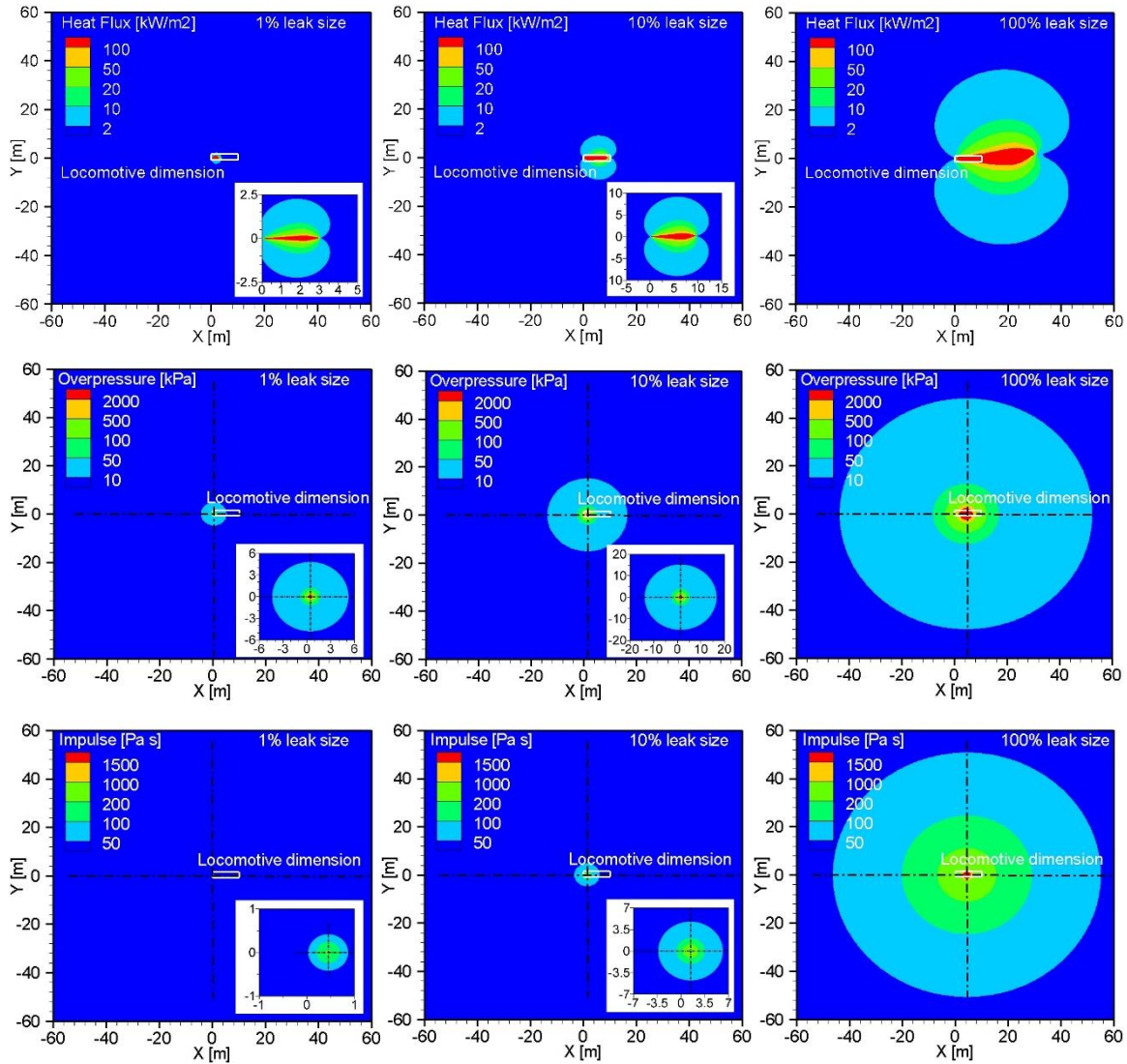
Figure 2 Event outcomes, top row: heat flux (kW·m^{-2}), middle row: overpressure (kPa), and bottom row: impulse (Pa·s) for leak sizes of 1%, 10%, and 100% from a ¾″ OD line containing H$_2$ at 350 bar. Black centrelines: overpressure and impulse origin; leak coordinates (0, 0).

3.1.2 Frequencies

Figure 3 compares the random component leak frequencies of the components at different leak sizes [3]. While valves have the highest leak frequencies at smaller leak sizes, filters consistently have relatively high leak frequencies at all sizes. Before reaching the 100% leak size stage, the component should go through smaller leak sizes (e.g., 1%). Such significant failure (100% leak size) happens gradually over time in the absence of accidents. Validated standard operating procedures, scheduled routine inspections, corrective and preventative maintenance procedures, and operating equipment within its recommended service life and the manufacturer's allowable limits will help to prevent such catastrophic leaks. The sum of random leak frequencies for all components at a leak size is the annual combined leak

frequency at that leak size. Table 5 summarizes these combined leak frequencies from all components at each leak size.
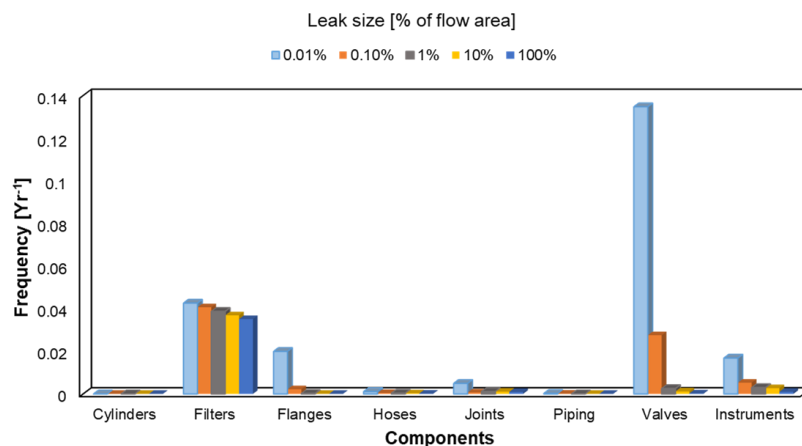

Figure 3 Annual random components leak frequencies as a function of leak sizes.

As stated earlier, a 100% leak size frequency combines random component leak frequencies, shutdown failures, and drive-offs (during refuelling) frequencies. At the given refuelling rate (Table 3), the combined shutdown failure and drive-off frequency is 3.46×10^{-6} per year. This frequency is nearly four orders lower than the total random component leak (3.74×10^{-2} per year). Using breakaway couplings prevents drive-off release and installing manually and remotely activated master shut-off valve(s) immediately adjacent to the gas storage prevents nozzle failure release [2].

The probabilities for the events of all the leak sizes are summarized in Table 5. The mass flow rate was calculated based on the leak size and the system pressure. The product of event probabilities and combined annual leak frequency at a given leak size is the total event frequency at that leak size. Of all 0.01% leak incidents, the probability for immediate ignition is only 0.08%. For 100% leak incidents, it is approximately seven times more (0.53%). While the frequency for a 100% leak is the lowest, it has the highest probability for immediate ignition. Also, the probability of immediate ignition is twice that for delayed ignition at all leak sizes [4]. So, the jet fire from immediate ignition having the higher frequency should contribute most to the fatality rate. Thus, when a leak happens, the fatality is expected to be maximum from a jet fire from a 100% leak size (longest hazard distance). To reduce the jet fire risk, immediate detection and isolation of leaks are crucial. This case study considers that 90% of all leaks will be detected and isolated (automatic shutdown event). Thus, the automatic shutdown has the highest frequency at all leak sizes, followed by a no ignition event for this case study.

Table 5 Event probabilities for the locomotive based on the hydrogen mass flow rate

Leak Size, % of flow area	Hydrogen Release Rate (kg/s)	Leak frequency [Yr^{-1}]	Ignition Probability		Shutdown Probability	No Ignition Probability
			Immediate	Delayed		
0.01	0.0003	0.221	0.0008	0.0004	0.9	0.0988
0.1	0.003	0.077	0.0008	0.0004	0.9	0.0988
1	0.028	0.046	0.0008	0.0004	0.9	0.0988
10	0.276	0.042	0.0053	0.0027	0.9	0.0920
100	2.765	0.037	0.0053	0.0027	0.9	0.0920

3.1.3 Consequences

Without considering the event probabilities, applying probit Equations (3) and (4) to heat flux and overpressure-impulse profiles gives the fatality probability from jet fire and explosion, respectively. Two sequential events must precede the jet fire after a leak: (1) leak not detected and isolated (no shutdown) and (2) immediate ignition. Therefore, when the product of the probabilities of these two

8

events (Table 5) is multiplied by the fatality probability, it gives the overall thermal fatality probability at a leak size. There is a third event probability for overpressure fatality: the probability of not immediately igniting after a leak not being detected and isolated. Table 6 summarizes hazard distances for jet fire and explosion, before and after considering event probabilities. Figure 4 illustrates examples of the reduction in thermal (Figure 4 top row) and overpressure (Figure 4 bottom row) fatality probabilities from a jet fire and an explosion for a 100% leak size after considering event probabilities.

Table 6 Hazard distances for jet fire and explosion before and after including event probabilities

Leak size [% of flow area]	Hazard Distance [m] for Thermal Fatality Probability ≥ 0.9		Hazard Distance [m] for Overpressure Fatality Probability ≥ 0.9	
	Before including event prob.	After including event prob.	Before including event prob.	After including event prob.
0.01	0.5	Negligible	Negligible	Negligible
0.1	1	Negligible	Negligible	Negligible
1	3	Negligible	Negligible	Negligible
10	9.5	Negligible	2.3	Negligible
100	30	Negligible	7.8	Negligible

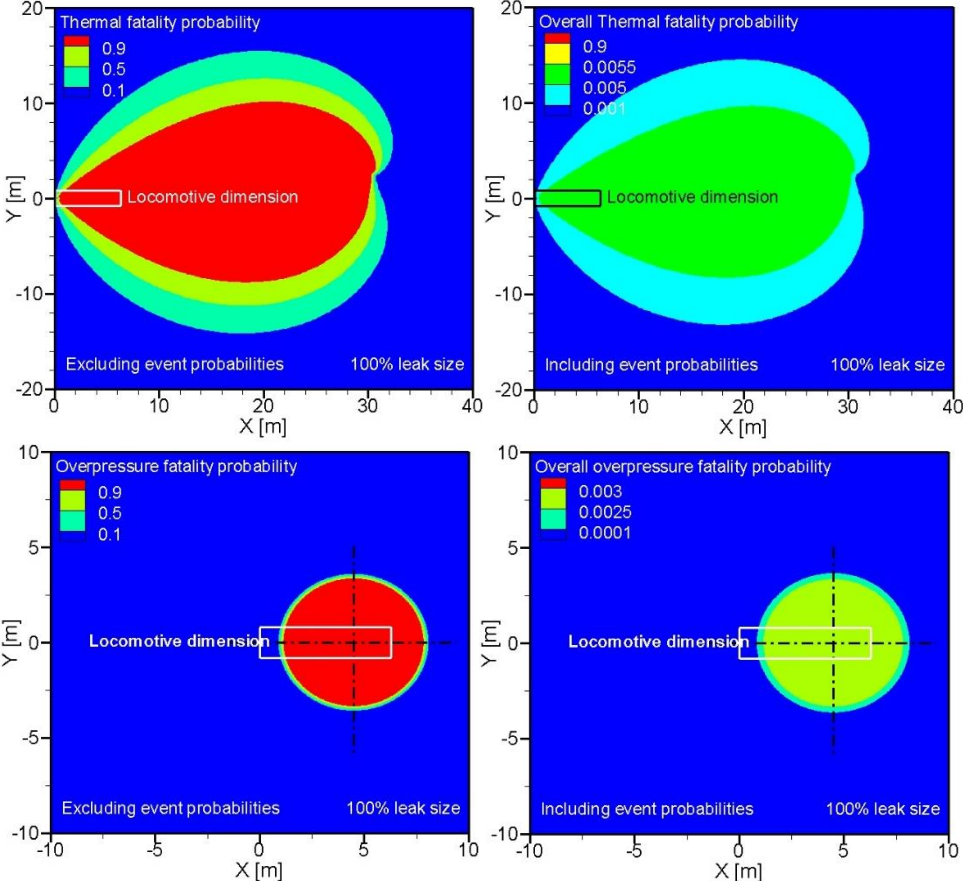Negligible: maximum fatality probability ≪ 0.9

Figure 4 Fatality probability of an occupant from a jet fire (top) and an explosion (bottom) from a 100% leak size, before (left) and after (right, overall fatality probability) considering probabilities of leak non-detection and immediate/delayed ignition with the fatality probability. Black centrelines: overpressure and impulse origin; leak coordinates (0, 0).

3.1.4 Risk Metrics

The risk metrics for four cases are compared in this section; Case 1 is the base case. The sensitivity parameters for these cases are listed in Table 7. The AIR results for cases 1–3 are shown in Figure 5.

Table 7 Sensitivity parameters of case studies and results

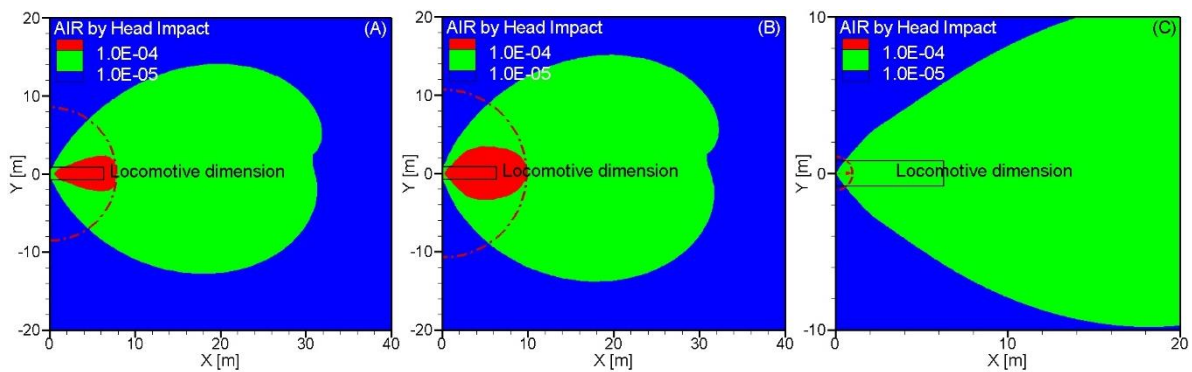| Case #	Number of occupants	Probability of leak and isolating detection	Random frequency for 100% leak size [Yr⁻¹]	Separation distance [m]
Case 1	1	0.9	0.037	7.8
Case 2	1	0.8	0.037	9.8
Case 3	1	0.9	0.012	1.0
Case 4	1-4	0.9	0.037	-

Figure 5 AIR profiles for (A) Case 1 (B) Case 2, and (C) Case 3 for a leak in a ¾″ OD pipe containing hydrogen at 350 bar. Separation distance marked by red semi-circle.

Figure 5A illustrates Case 1 or the base case scenario. With a leak detection and isolation probability of 90%, the probability for immediate and delayed ignitions ranged from 0.08–0.5% and 0.04–0.3%, respectively, depending on the leak size. The safe separation distance was 7.8 m from the leak.

Case 2 (Figure 5B) depicts AIR sensitivity to immediate leak detection and isolation, illustrating its importance in lowering the risk and safe separation distance. With a 10% reduction in leak detection and isolation probability (from 90% to 81%), the probability for immediate and delayed ignitions ranged from 0.2–1% and 0.1–0.5%, respectively, depending on the leak size. These fatal events probabilities nearly doubled when compared with the base case probabilities. The safe separation distance increased from 7.8 m to 9.8 m from the leak.

Case 3 (Figure 5 C) illustrates AIR sensitivity toward random component leak frequency. Even with a high probability of detecting and isolating a leak (90%), the safe separation distance extended beyond the longest locomotive dimension (6.3 m). In the absence of an accident or sabotage, the highly damaging 100% leak is not expected to occur all of a sudden. Normal equipment wear and tear may initially result in small leaks, which without remedial measures, can progress to larger ones gradually. These leaks could eventually result in a damaging rupture (100% leak size) if not rectified. Routine testing (detection system) and equipment maintenance can prevent a significant leak event by identifying, fixing, and preventing the recurrence of minor leaks much before it reaches 100%. By reducing the random leak frequency for the 100% leak size by half-order $\left(\frac{1}{\sqrt{10}} \text{ times}\right)$, the safe separation distance decreased from 7.8 m to 1 m. The probabilities of all the events remained the same as in the base case.

Case 1, Case 2, and Case 3 represent single occupant's risk due to a leak in a hydrogen system. Case 4 analyzes the effect of the number of occupants on risk metrics using Base Case conditions. In a hydrogen locomotive, only employees and contractors are expected to be present to keep risks low and avoid fatalities. Practically, the occupants will be in close proximity to each other, spending nearly an equal amount of time together. Hence, the probability of fatality for all will be nearly the same. Figure 6 (left) illustrates one representative example. For an occupant, their position is represented by P-1. If there is a second person, their position is given by P-2. Similarly, the third and fourth persons are depicted by P-3 and P-4 for a total occupancy of three and four, respectively. The basis for the distance between the occupants (0.3 m radius around P-1) is half the CHIC recommended minimum clearance for equipment repairs and replacements [2]. Figure 6 (right) shows that the PLL increases with the number of occupants, while AIR values are close (9.5% coefficient of variance) to average values of multiple occupants scenarios. The risk metrics have been reverified using HyRAM for the toolkit validation.
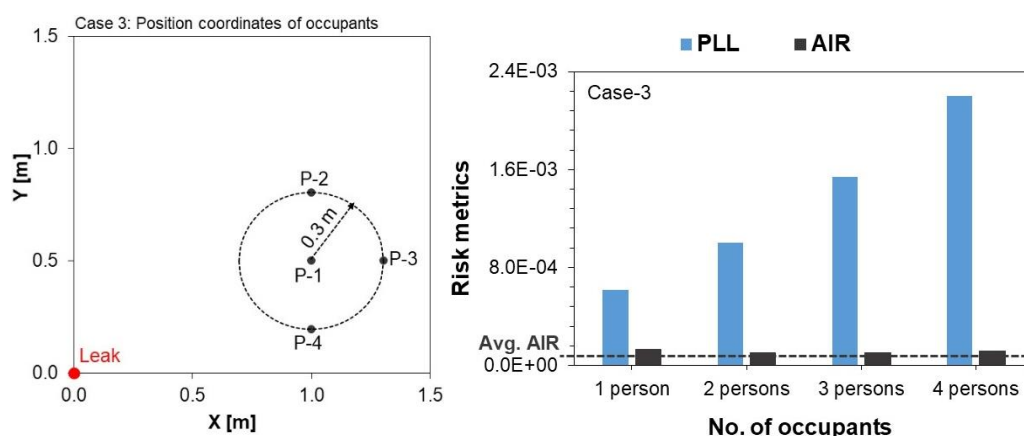

Figure 6 Left: occupants position coordinates around the leak; Right: Case 4 risk metrics as a function of number of occupants in the vicinity of a leak in a ¾″ OD pipe containing hydrogen at 350 bar.

4. CONCLUSION

Using CNL's toolkit, QRA for a hydrogen locomotive was carried out by applying deterministic and probabilistic approaches to the physical outcomes of events following a leak. The physical outcomes of events (jet fire, explosion) following the leak were quantified using analytical models. The hazard distances up to which an occupant can be exposed to the threshold values of these outcomes were validated with HyRAM. The consequences for these outcomes were calculated as the fatality probability using probit equations. However, the ultimate fatality probabilities are lower due to the low probability of event occurrences.

The probability that a leak detection sensor immediately detects and isolates a leak is crucial. This probability gives shutdown frequency, an event that immediately reduces the risk to the life of the occupants and prevents structural damage. In addition to using these sensors, implementing a corrective and preventive action (also known as CAPA in quality management) plan can prevent the most damaging leak incident and stop the recurrence of smaller, less dangerous leaks (such as routine scheduled maintenance of the components). The risk-informed approach helps reduce the cost of hydrogen technology deployment and gives confidence regarding the safety of hydrogen installations to authorities and industries.

The toolkit in its present state can be used for the gaseous hydrogen only. The toolkit will be updated to include liquid hydrogen, other gases (e.g., methane, carbon monoxide), and blends (e.g., hydrogen with methane or carbon monoxide). Results from the computational fluid dynamics modeling of experimental data from CNL's laboratories' experiments will be appended to the toolkit, such as new/updated physics models and numerical parameters required for QRA estimated by modeling.

11

5. ACKNOWLEDGEMENTS

6. REFERENCES

[1] "Hydrogen Strategy for Canada, Seizing the Opportunities for Hydrogen, A Call to Action," Natural Resources Canada, 2020. [Online]. Available: https://natural-resources.canada.ca/sites/nrcan/files/environment/hydrogen/NRCan_Hydrogen-Strategy-Canada-na-en-v3.pdf.

[2] BNQ, "Canadian Hydrogen Installation Code," Bureau de normalisation du Québec, 2022.

[3] B. D. Ehrhart, E. S. Hecht and K. M. Groth, "Hydrogen Risk Assessment Models (HyRAM) Version 4.1 Technical Reference Manual," Sandia National Laboratories, 2022.

[4] A. Tchouvelev, R. Hay and P. Benard, "Comparative risk estimation of compressed hydrogen and CNG refuelling options," Canadian Hydrogen Association workshop on building Canadian strength with hydrogen systems Proceedings, Canadian Hydrogen Association.

[5] T. Skjold, D. Siccama, H. Hisken, A. Brambilla, P. Middha, K. Groth and A. LaFleur, "3D risk management for hydrogen installations," International Journal of Hydrogen Energy, vol. 42, no. 11, pp. 7721-7730, 2017.

[6] H.-R. Gye, S.-K. Seo, Q.-V. Bach, D. Ha and C.-J. Lee, "Quantitative risk assessment of an urban hydrogen refueling station," International Journal of Hydrogen Energy, vol. 44, no. 2, pp. 1288-1298, 2019.

[7] B. Ehrhart, S. Harris, M. Blaylock, A. Muna and S. Quong, "Risk assessment and ventilation modeling for hydrogen releases in vehicle repair garages," International Journal of Hydrogen Energy, vol. 46, no. 23, pp. 12429-12438, March.

[8] M. Hirayama, Y. Ito, H. Kamada, N. Kasai and T. Otaki, "Simplified approach to evaluating safety distances for hydrogen vehicle fuel dispensers," International Journal of Hydrogen Energy, vol. 44, no. 33, pp. 18639-18647, 2019.

[9] E. A. Saltanaeva and A. V. Maister, "Optimization of calculations of the effects of spill fires during accidents on linear equipment," E3S Web of Conferences, vol. 140, no. 07002, 2019.

[10] A. Birch, D. Hughes and F. Swaffield, "Velocity Decay of High Pressure Jets," Combustion Science and Technology, vol. 52, pp. 161-171, 1987.

[11] W. Houf and R. Schefer, "Predicting radiative heat fluxes and flammability envelopes from unintended releases of hydrogen," International Journal of Hydrogen Energy, vol. 32, no. 1, pp. 136-151, 2007.

[12] G. Hankinson and B. J. Lowesmith, "A consideration of methods of determining the radiative characteristics of jet fires," Combustion and Flame, vol. 159, pp. 1165-1177, 2012.

[13] M. Tang and Q. Baker, "A New Set of Blast Curves from Vapor Cloud Explosion," Process Safety Progress, vol. 18, no. 4, pp. 235-240, 1999.

[14] K. M. Groth, J. L. LaChance and A. P. Harris, "Early-Stage Quantitative Risk Assessment to Support Development of Codes and Standard Requirements for Indoor Fueling of Hydrogen Vehicles," Sandia National Laboratories, 2012.

[15] J. LaChance, A. Tchouvelev and A. Engebo, "Development of uniform harm criteria for use in quantitative risk analysis of the hydrogen infrastructure," International Journal of Hydrogen Energy, vol. 36, p. 2381–2388, 2011.